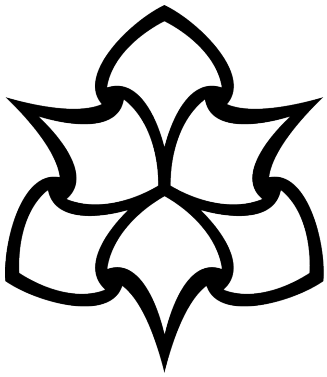

Differential Responses of Myoblasts and Myotubes to Photobiomodulation are associated with Mitochondrial Number.

H. Serrage[1,2,3]*, S. Joanisse[2], P. R. Cooper[1], W. Palin[1], M Hadis[1], O. Darch[3], A. Philp[2,4], M. R. Milward[1]

School of Dentistry, University of Birmingham, UK [1]

School of Sport, Exercise and Rehabilitation Sciences, University of Birmingham, UK[2]

Philips Research, Eindhoven, Netherlands[3]

Garvan Institute of Medical Research, Sydney, Australia[4]

Corresponding author details*:
Email address: HJS535@student.bham.ac.uk
Address: Birmigham Dental Hospital, 5 Mill Pool Way, Birmingham, West Midlands, UK, B5 7EG

Abstract

Objective: Photobiomodulation (PBM) is the application of light to promote tissue healing. Current indications suggest PBM induces its beneficial effects *in vivo* through upregulation of mitochondrial activity. However, how mitochondrial content influences such PBM responses has yet to be evaluated. Hence, the current study assessed the biological response of cells to PBM with varying mitochondrial contents.

Methods: DNA was isolated from myoblasts and myotubes (differentiated myoblasts) and mitochondrial DNA (mtDNA) was amplified and quantified using a microplate assay. Cells were seeded in 96-wellplates, incubated overnight and subsequently irradiated using a LED array (400nm, 450nm, 525nm, 660nm, 740nm, 810nm,830nm and white light, 24mW/cm², 30-240s, 0.72-5.76J/cm²). The effects of PBM on markers of mitochondrial activity including reactive-oxygen-species (ROS) and real-time mitochondrial respiration (Seahorse XFe96) assays were assessed 8 h post-irradiation. Datasets were analysed using general linear model followed by one-way ANOVA (and post hoc-Tukey tests); p=0.05).

Results: Myotubes exhibited mtDNA levels 86% greater than myoblasts ($p<0.001$). Irradiation of myotubes at 400nm, 450nm or 810nm induced 53%, 29% and 47% increases (relative to non-irradiated-control) in maximal respiratory rates respectively ($p<0.001$). Conversely, irradiation of myoblasts at 400nm or 450nm had no significant effect on maximal respiratory rates.

Conclusion: This study suggests that mitochondrial content may influence cellular responses to PBM and as such explain the variability of PBM responses seen in the literature.

Key words: *Low level light therapy, LLLT, Photobiomodulation, Myogenesis, mitochondria.*

This article has been accepted for publication and undergone full peer review but has not been through the copyediting, typesetting, pagination and proofreading process, which may lead to differences between this version and the Version of Record. Please cite this article as doi: 10.1002/jbio.201800411

1 Introduction

Photobiomodulation (PBM) is a non-invasive treatment that utilises light at a power output less than 500mW at wavelengths from 400-1100 nm to promote tissue healing, reduce inflammation and induce analgesia (1). Over 800 publications have reported the efficacy of PBM in treating an array of musculoskeletal conditions including subacute and chronic low back pain (2) and exercise induced muscle fatigue (3). Musculoskeletal disorders relate to an array of conditions that affect movement and are a significant burden; not only to the affected individual but also to healthcare systems due to the costs associated with management. Indeed, a report by the World Health Organisation concluded that up to 33% of the population are affected by lower back pain at any given time (4).

Despite the positive evidence surrounding the use of PBM in treating musculoskeletal conditions, controversy still surrounds its application in practice due to a lack of consistency in the recording of treatment parameters. Notably a number of key irradiation parameters should be reported including wavelength (nm) and irradiance (mW/cm^2), amongst others (5). These parameters are often either misreported or not reported at all making it difficult to compare literature currently published.

Another key caveat in the use of PBM is the lack of knowledge as to how light energy elicits its beneficial molecular effects. Current literature indicate light acts directly upon the mitochondrial electron transport chain (ETC), specifically complex IV (6). The ETC is formed of five complexes and its main purpose is to produce adenosine triphosphate (ATP); the cells energy source. It is understood that photons of light at wavelengths including 810nm excite complex IV, causing the dissociation of nitric oxide (NO) from its binding site, allowing oxygen to bind in its place and therefore allowing the progression of the ETC (6, 7). As the ETC progresses, complexes I and III of the chain also produce reactive oxygen species (ROS). The production of ROS and ATP then induce the activation of transcription factors and subsequent gene expression changes including increased nuclear factor E2-related factor 2 (Nrf2) (8), a gene whose expression is commonly associated with increased mitochondrial biogenesis (9).

Many studies report the effect of PBM on mitochondrial activity through the use of surrogate assays including ROS (10) and ATP (11) generation. However, despite wide evidence supporting this ideology, no studies to date report the effects of PBM on mitochondrial respiration or whether mitochondrial number can influence response to PBM. In fact, the number of mitochondria per cell can vary from 80-2000 dependent upon the cell type explored (12). *Robin and Wong* reported that there are approximately 1000 mitochondria per liver cell whilst there are around 300 mitochondria per human lung fibroblast cell (13).

This study aimed to firstly characterise a system that could be employed to evaluate the effects of PBM on changes in mitochondrial respiration in real time and secondly to determine the optimal treatment parameters that elicit a molecular response in muscle-derived cells in which mitochondrial activity is key to their behaviour. C2C12 myoblasts have been suggested to be an appropriate model for mimicking the process of skeletal muscle cell differentiation *in vitro* (14). When exposed to appropriate conditions myoblasts differentiate into myotubes *in vitro* (15). Mature myotubes are cited to have a higher population of mitochondria than myoblasts (16, 17). Hence, myoblasts and myotubes were employed to determine whether cells with a higher mitochondrial population responded differently to PBM.

2 Methods

2.1 LED array characterisation

2.1.1 Spectral characterisation

A UV-Vis spectrometer (USB4000, Ocean Optics, UK) coupled to a 200µm optical fibre and 3.9mm cosine corrector and calibrated to (National Institute of Standards and Technology) NIST standards was employed to assess the spectral irradiance and wavelength delivered at the base of each individual culture well (n=6). Absolute irradiance was determined from the integral of the spectral irradiance (380-880nm). Further detail outlining spectral characterisation methods, LED array design and selection of wavelengths are described by *Hadis et al* (18).

2.1.2 Beam Profile

A charge coupled device (CCD) beam profile camera (SP620, Ophir, Spiricon, Israel) was employed to measure spatial distribution of power emitted from each LED in the array. A 50mm CCTV lens (Ophir, Spiricon, Israel) was attached to the camera and focused on the base of each well. Following linear, optical and ambient light correction, images were recorded using BeamGage software (Ophir, Spiricon, Israel). Detailed experimental procedure has previously been reported by *Hadis et al (18).*

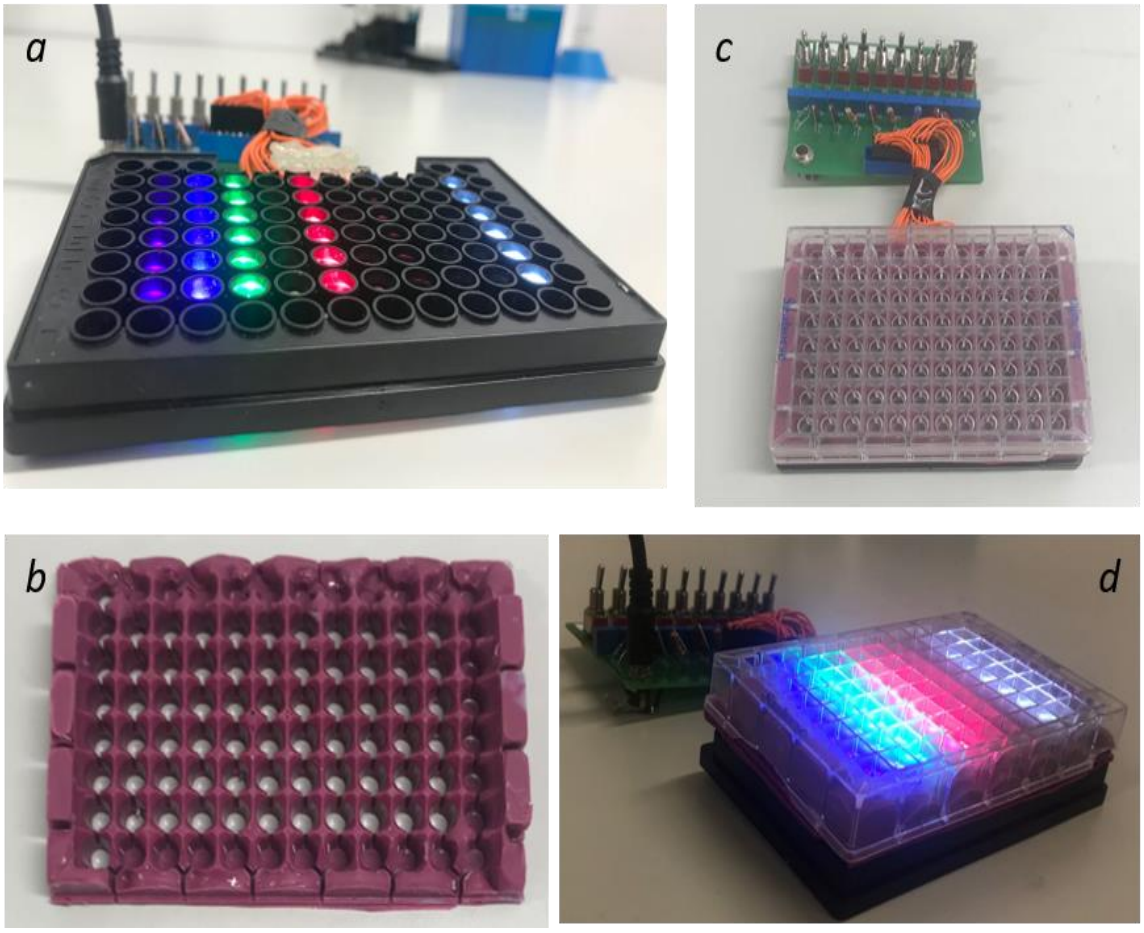

Figure 1: a) Shows LED array without any plate b) shows mask constructed from silicon, c) shows seahorse XFe96 microplate plate fitted with mask on top of LED array d) shows Seahorse XFe96 microplate fitted with mask placed on LED array when on (all wavelengths). All spectral characterisation experiments were undertaken with the seahorse plate fitted with mask placed directly above the LED array, ensuring concentric alignment with LEDs beneath.

2.2 Biological responses

2.2.1 Myoblasts culture

A mouse myoblast cell line (C2C12 (ATCC® CRL-1722™), ATCC, LGC standards, UK, passage 8-11) (14) were cultured in monolayers in Dulbecco's modified eagle medium (DMEM, Gibco, UK) supplemented with 10% v/v FCS, 1% v/v penicillin/streptomycin (P/S) and 1% v/v L-glutamine (Sigma-Aldrich, UK). Cells were seeded into 96-well black clear bottom plates (7000cells/well (Sigma-Aldrich, UK)) and Seahorse XFe96 plates (10,000cells/well (Agilent, UK)) , incubated overnight (37^{o}c, 5% CO_2), irradiated as described in *2.2.3* and changes in mitochondrial activity were assessed 8 or 24hrs post-irradiation.

2.2.2 Myotube differentiation

Myoblast cultures were seeded into Seahorse XFe96 plates as described in section 2.2.1 and ~70% confluency was reached, cultures were washed with PBS and differentiation media was subsequently applied which contained phenol red free DMEM containing 2% v/v horse serum and 1% v/v sodium pyruvate (Sigma-Aldrich, UK) to induce differentiation for six days. Myotubes were then irradiated as described above and changes in mitochondrial activity were assessed 8hrs post irradiation.

2.2.3 Array characterisation for Seahorse XF cell mitochondrial stress assay (Agilent, UK).

A Seahorse XFe96 Analyser (Agilent Technologies, UK) was employed to measure the cells oxygen consumption rate (OCR) as a marker of mitochondrial respiration. One-hour prior to undertaking the assay, culture media was aspirated, cells washed with phosphate buffered saline (PBS) three times and Seahorse XF assay media (25mM glucose, 1mM pyruvate and 2mM glutamine (Agilent, UK)) was applied and equilibrated in a CO_2 free incubator (INCU-line®, VWR, UK). Compounds altering mitochondrial activity were then applied to the system including: Oligomycin (inhibits complex V of the ETC, 1µM), carbonyl cyanide-4(triflouromethoxy)phenylhydrazone (FCCP, uncoupling agent induces respiration to be undergone at maximal rates, 2µM), antimycin and rotenone A (inhibit complexes I and III, inhibiting ETC activity, 0.5µM). Subsequently the plate was placed in a Seahorse XFe96 analyser (Agilent, UK) and compounds were sequentially injected into the system to induce changes in ETC activity. The Seahorse analyser then measured changes via assessment of oxygen consumption rate in real-time (OCR, pmol/min). OCR values were subsequently normalised for protein content in individual wells. Protein concentration was determined using DC protein assay (Bio-rad, USA). This enabled calculation of individual parameters including basal respiration, maximal respiration, ATP production, spare respiratory capacity and non-mitochondrial respiration (8). During analysis, values for non-mitochondrial activity were subtracted from values evaluating the effects of PBM directly on mitochondrial activity. This provided a further control step ensuring results would reflect the effects of PBM on mitochondrial activity only.

An opaque dental silicone impression material (Impregum™ Penta Soft, 3M, USA) mask (*Figure 1b*) was created to ensure uniform irradiation of *in vitro* cultures and to eliminate light bleed at the base of wells where cells adhere (*Figure 1c and 1d*). The distance between the LEDs and specimen surface was fixed at 3mm in each well. The spectral irradiance and beam profile of each diode were evaluated with the mask fitted to a Seahorse microplate *(Figure 1d).* Characterisation was then undergone as described in section *2.1.* The effects of PBM were evaluated at wavelengths spanning the visible and near infra-red spectra (400-830nm) at irradiation periods between 30-240s and an irradiance output of 24mW/cm² to achieve radiant exposures of 0.72-5.76J/cm².

2.2.4 Mitochondrial DNA (mtDNA) quantification

A REPLI-g® mitochondrial DNA kit (Qiagen, UK) was used to amplify mtDNA in whole DNA samples isolated from cell cultures. Sample DNA concentrations were measured spectrophotometrically (Eppendorf biophotometer, Eppendorf, UK) and diluted accordingly to contain 10ng/µl of DNA. Amplification of mtDNA was then undertaken according to the manufacturer's protocol.

To assess mtDNA quantities in cell supernatants, initially a standard curve was generated using calf thymus DNA at a maximal concentration of 10ng/µl. SYBR® Safe DNA gel stain (10,000x concentrate, Invitrogen, UK) was diluted in TAE buffer at 1:1250. Samples and standards were then combined at 2% v/v with the dilute SYBR® Safe dye and incubated for 10 minutes (19). Fluorescence was measured using a fluorimeter (Twinkle LB 970, Berthold Industries Ltd, 485nm/535nm, excitation/emission respectively).

2.2.5 3-(4, 5-Dimethylthiazol-2-yl)-2,5-Diphenyltetrazolium Bromide (MTT) assay

To assess cell metabolic activity, an MTT assay (Sigma-Aldrich, UK) was utilised (20). MTT was dissolved in PBS at 0.05g/ml and aliquoted at 15µl/well 8/24h post irradiation and incubated for 4h at 37°c. MTT solution was aspirated and replaced with 50µl/well of dimethyl sulphoxide (DMSO, Sigma-Aldrich, UK). Absorbance was read at 570nm using a micro-plate reader (ELx800 Universal Microplate reader, Bio-Tek Instruments, UK).

2.2.6 Reactive Oxygen Species (ROS) assay

ROS formation was assessed using 2', 7'-dichlorodihydrofluorescein diacetate (H_2DCFDA) fluorescent probe (Thermo-Fischer Scientific, UK). Free radicals catalyse the conversion of H_2DCFDA to its fluorescent bi-marker DCF, enabling quantification of ROS production. At 8h post-irradiation media was aspirated, cells were washed with phosphate buffered saline (PBS) and were treated with 10µm H_2DCFDA and incubated for 1 hour at 37°C (22). Fluorescence was read using a fluorimeter as described in section *2.2.4*.

2.3 Statistical analysis

Data was processed utilising Excel software (Microsoft) and analysis was performed using SigmaPlot software (Systat Software Inc, UK). All data was analysed using a GLM followed by one-way ANOVA test followed by a Tukey test to determine significant differences between non-irradiated controls and light treated groups *($p<0.05$)*.

3 Results and Discussion

3.1 Characterisation of LED arrays for use in Seahorse assays.

LED arrays provide a high-throughput approach for analysis of multiple parameters and their effects *in vitro*. The current study first aimed to characterise a system that could be employed for use with the Seahorse XFe96 analyser system.

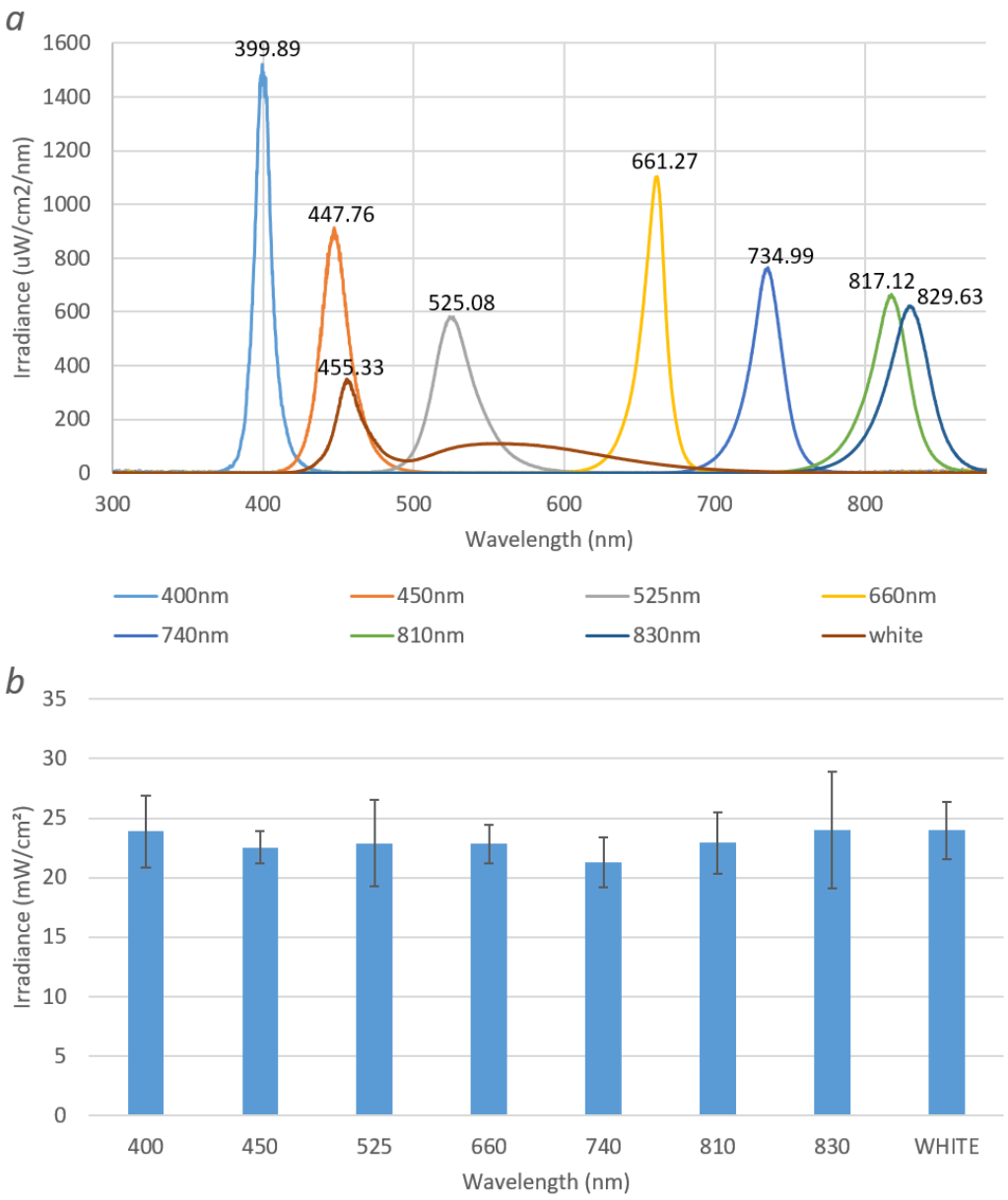

Figure 2: Array spectral characterisation data where a) Spectral irradiance values of LED channels in the array (n=6), b) average absolute irradiance in each channel (n=6).

Table 1: Indicates values of emitted wavelengths, spectral irradiance and radiant exposure after irradiation periods ranging between 30s-240s

	Radiant exposure (J/cm²)			
Wavelength (nm)	**30s**	**60s**	**120s**	**240s**
399.89±1.55	0.72	1.43	2.86	5.73
447.76±1.69	0.68	1.35	2.70	5.41
525.08±1.25	0.69	1.37	2.75	5.50
661.27±0.56	0.68	1.37	2.74	5.48
734.99±1.21	0.64	1.28	2.55	5.11
817.12±0.64	0.69	1.37	2.75	5.50
829.63±2.64	0.72	1.44	2.88	5.76
455.33±0.11	0.72	1.44	2.87	5.75
AVERAGE:	*0.69±0.03*	*1.38±0.05*	*2.76±0.10*	*5.53±0.21*

A mask constructed from silicon was designed to surround each well of the plate, preventing bleed between wells to ensure only a single wavelength of light would impact the biological response in each well-culture. Spectral characterisation undertaken to confirm wavelength and spectral irradiance values were consistent with those used in previous studies employing different plate formats (23). Data indicated the array employed for in vitro studies emitted wavelengths ranging from 400-830nm (*figure 2a)* and an average irradiance of 23.05mW/cm² *(figure 2b).* These data also confirmed there was no bleed of light between LED columns where *figure 2a* indicates LEDs exhibited only a single peak of the expected wavelength and *figure 2b* shows there was no significant difference in irradiance output from one wavelength to the next. Similar irradiance values have also been used in studies exploring the effect of PBM on myoblast function (see *supplementary table 3* for examples (24, 25)). *Table 1* indicates radiant exposure values, in which there is no significant difference from one wavelength to the next (irradiation parameters and the effects of PBM on media temperature are further elucidated in *supplementary figure 1, figure 2* and *table 1*). Hence the data confirms the accurate delivery of key radiometric parameters without confounding effects such as temperature.

Another key parameter to be considered was that of the beam profiles of each LED utilised in this array. LEDs employed in this array exhibit a typical Gaussian distribution of light (*figure 3a,* indicates a single representative from each wavelength channel) in which spectral irradiance is most intense in the central area and becomes more diffuse towards the edges of the beam area (26). *Table 2* indicates LEDs emitting a wavelength of 525nm exhibited a significantly smaller ($p<0.05$) beam area and power output than LEDs emitting wavelengths of 400nm and 660nm, whilst there was no significant difference at all other wavelengths. In this particular experimental set-up, the LED array was designed to enable alignment of LEDs with the plate directly above at a specific irradiance value. As described by *Hadis et al* (18) that whilst there is variability in the homogeneity of each LED, the effects of this have been minimised through ensuring there is no significant difference in the output of a series of parameters including irradiance (mW/cm²) and radiant exposure (J/cm²).However, despite this it will be important to take into account the effects this may have on the biological output of our experiment. These data indicate the importance of evaluation of beam area.

The data obtained for array characterisation indicates its suitability for use in subsequent *in vitro* assay application.

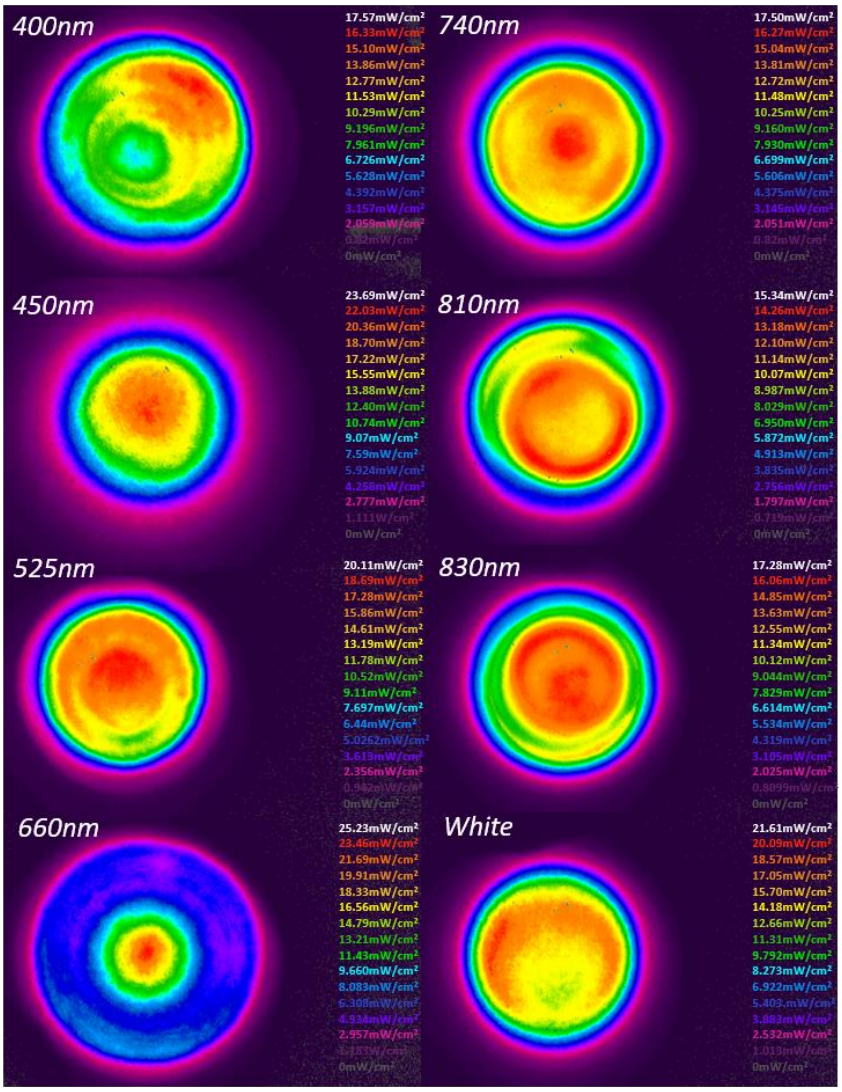

Figure 3: Demonstrates spatial distribution of irradiance of LEDs emitting each wavelength on the array. Images were taken in the plane of a target screen placed over the array surface to enable accurate measurement of beam diameter using BeamGage software. The target screen was placed at the same distance away from the array as a Seahorse XFe96 plate. Whilst the target screen could not be incorporated with the plate in place supplementary figure 3 and table 1 indicate beam profiles, average beam areas and power output with the plate in place.

Table 2: indicates differences in average beam area and power output emitted from one wavelength to the next. Means that do not share the same letter are significantly different, in which LEDs emitting wavelengths of 400nm and 660nm (A) exhibit significantly larger beam areas and power outputs than LEDs emitting 525nm light (B, p=<0.05). Average beam area was calculated from diameters provided from use of BeamGage software.

Wavelength (nm)	Average Beam area (cm²)	Power (mW)
400	0.370 ± 0.008^{A}	8.931 ± 0.184^{A}
450	0.337 ± 0.003^{AB}	8.484 ± 0.063^{AB}
525	0.257 ± 0.007^{B}	6.039 ± 0.157^{B}
660	0.364 ± 0.003^{A}	9.01 ± 0.068^{A}
740	0.298 ± 0.007^{AB}	6.834 ± 0.159^{AB}
810	0.335 ± 0.007^{AB}	7.688 ± 0.158^{AB}
830	0.307 ± 0.01^{AB}	7.453 ± 0.233^{AB}
White	0.291 ± 0.009^{AB}	7.721 ± 0.242^{AB}

3.2 The effects of PBM on mitochondrial activity

The second objective of this study was to evaluate the effects of PBM on mitochondrial activity of myoblasts and myotubes. Myotubes are reported to possess higher quantities of mitochondrial proteins and enzymes (27) and hence greater numbers of mitochondria. Whilst it is not feasible to directly measure number of mitochondria per cell due to the dynamic nature of mitochondria, mtDNA copy number has been correlated to mitochondrial content in previous studies (28). Hence, mtDNA was isolated from both myoblasts and myotubes and quantified. *Figure 4* provides evidence that myotubes possessed a greater ratio of mtDNA:nDNA compared with myoblasts *(p<0.05)*.

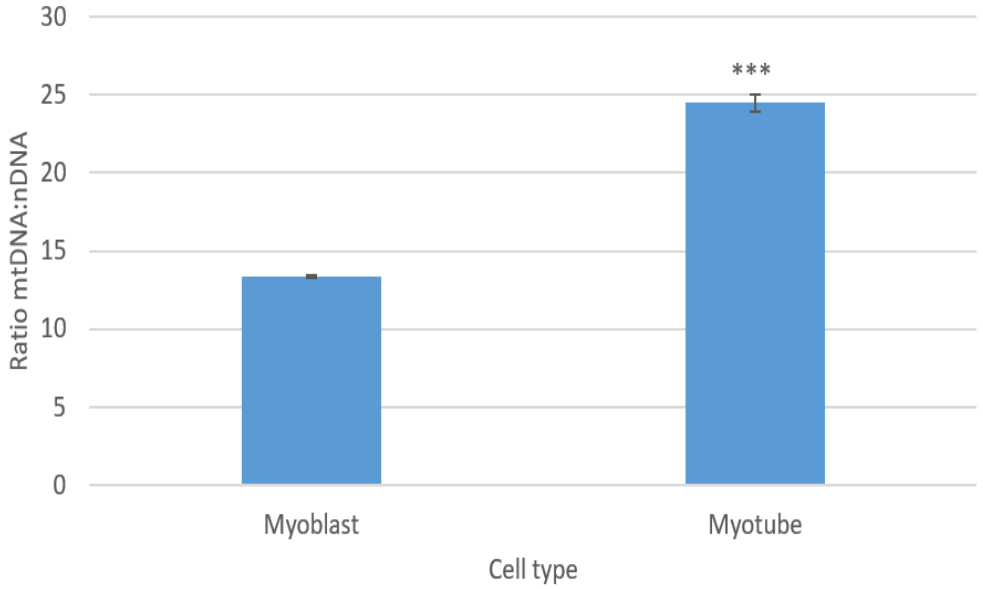

*Figure 4: Shows relative differences in the ratio of mtDNA:nDNA between myoblasts and myotubes (n=4 ,p8). Significance was assessed using a t-test (***=p<0.001).*

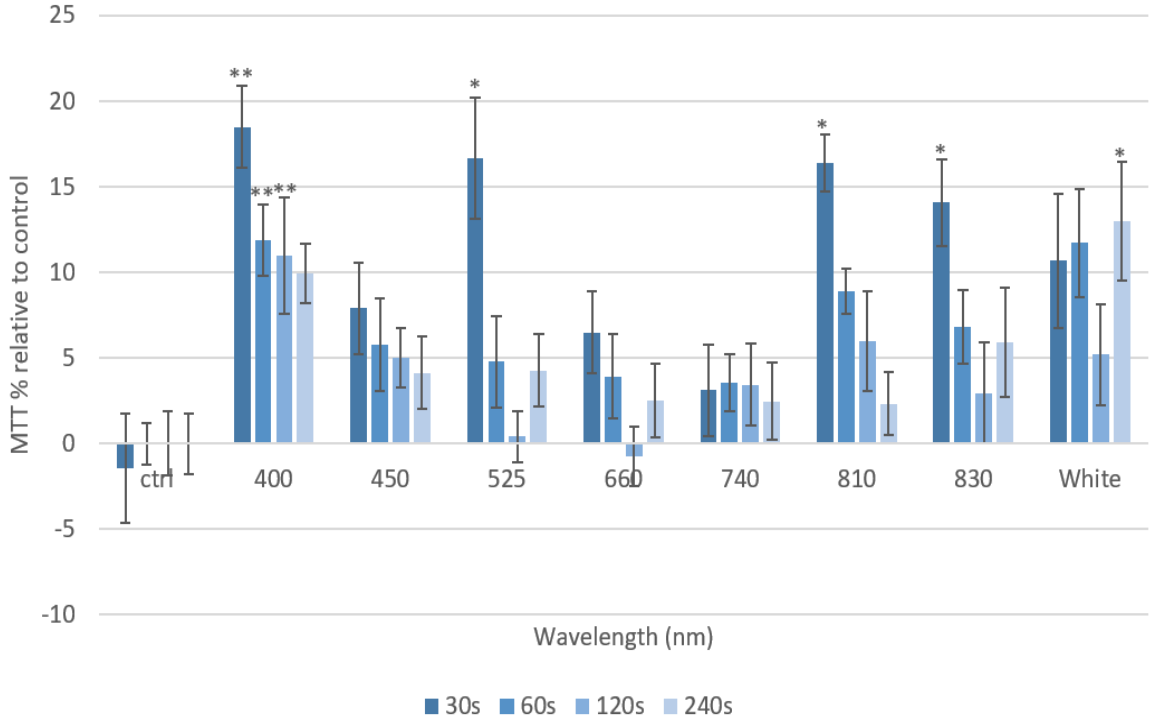

*Figure 4: Indicates high throughput analysis of wavelengths (400-830nm) and irradiation periods (30-240s) on cell metabolic activity of mouse myoblast cells (C2C12, n=12 replicates, 3 plates irradiated) (24mW/cm², 0.72-5.76J/cm², 30-240s). Significance is indicated by ***=p<0.001, **=p<0.01, *=p<0.05 relative to the non-irradiated control, where all data is shown as a percentage of the non-irradiated control. where the non-irradiated control was normalised to 0%.*

Therefore, an MTT assay was employed as a high-throughput method to examine the effects of a series of wavelengths (400-830nm) and irradiation times (30-240s) on cell metabolic activity of myoblasts 24hrs post irradiation. Irradiation for 30s at a wavelengths of 400nm and 810nm induced 18.46%, and 16.38% increases in cell proliferation respectively *(figure 5, p<0.05)*. Interestingly, white light induced a significant increase in cell proliferative capacity following irradiation for 240s whilst all other wavelengths proved to induce the greatest affect following a 30s irradiation period. This may be reflective of the differential biphasic dose response from one wavelength to the next where longer or shorter periods of irradiation could cause the most significant effects dependent upon the wavelength used. Also, white light is a combination of multiple visible light wavelengths and therefore the contribution of a single wavelength for any potential therapeutic effect within the white light band must be substantially reduced compared to the use of narrower wavebands at similar irradiance. It can also be noted that whilst wavelengths within the red spectra are commonly used in PBM research (620-750nm (29)), no effect on cell metabolic activity was measured here. This may be due to the homogeneity of the beam profile at 660nm *(figure 3)* or indeed as discussed above, the optimal range for red light to induce an effect was not reached in this experimental setup. Hence, further study will be required to determine whether irradiation at 660nm and with a more homogenous beam profile will influence biological output *in vitro.* Whilst other wavelengths

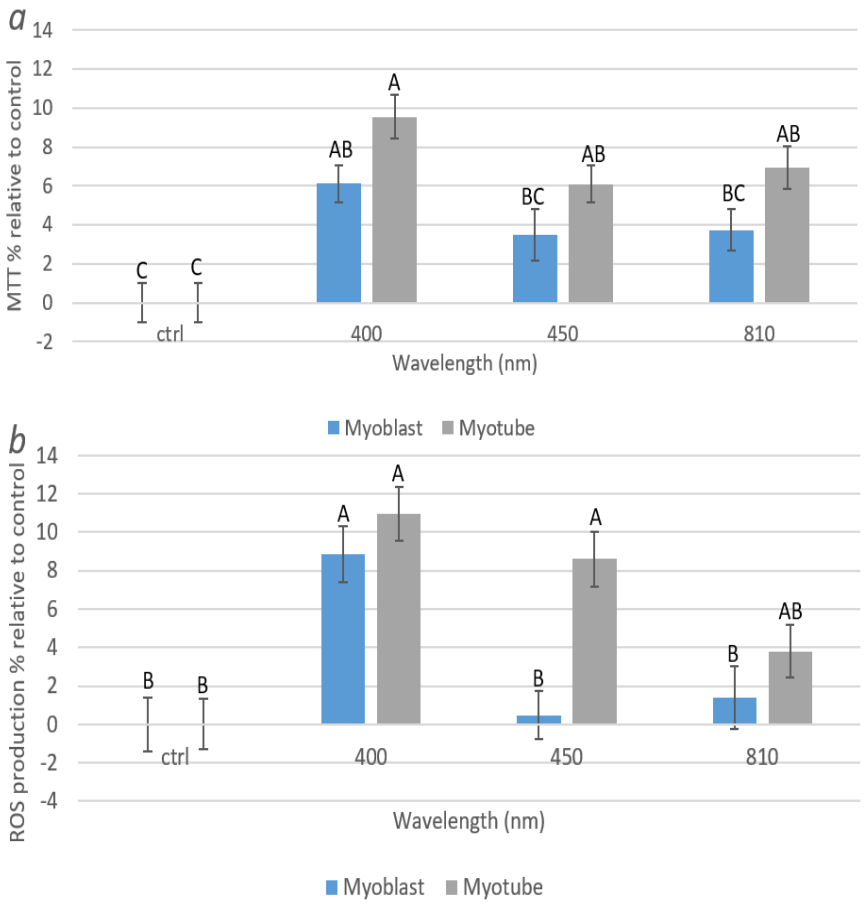

Figure 5: a) Shows effect of PBM on cell metabolic activity from myoblasts and myotubes (30s, 0.72J/cm², n=18, 3 plates irradiated) to wavelengths of 400, 450 and 810nm. b) Indicates the effects of PBM on ROS production from myoblasts and myotubes (30s, 0.72J/cm², n=18, 3 plates irradiated). The effects of PBM were evaluated 8hrs post-irradiation. Means that do not share the same letter are significantly different (p<0.05).

and irradiation periods proved effective in inducing a significant response from myoblasts, wavelengths of 400nm, 450nm and 810nm and an irradiation period of 30s was selected to compare the response of myoblasts and myotubes to PBM due to their efficacy in inducing a response from an array of other cell types previously studied (data not shown).

Once parameters were identified for further study a series of key markers for mitochondrial activity were explored 8hrs post irradiation. A period of 8hrs post irradiation was selected as a previous study indicated this time point post-irradiation induced the most significant and reliable changes in real time mitochondrial activity (supplementary *figure 4*, (1, 8 and 24hrs post irradiation were evaluated)). *Figure 6* indicates that whilst a wavelength of 400nm and irradiation period of 30s induced significant increases in markers for mitochondrial activity from myoblasts and myotubes, increases in the activities of these mitochondrial markers at all wavelengths were only observed in myotube cultures *($p<0.05$).* This may indicate that cells with higher mitochondrial content have increased responsivity to light. Interestingly, *Kushibiki et al* investigated the effect of PBM at wavelengths of 405nm and 808nm at 100mW/cm² on ROS production from C2C12 cells. They found that only violet-blue light upregulated ROS production whilst near infrared light had no effect. Our data provides similar findings, with a wavelength of 400nm inducing significant increases in ROS production from myoblasts (30). Some authors have also reported the effects of PBM in inducing myogenic differentiation from myoblasts to myotubes (31, 32). Hence, future work may involve evaluation of the effects of parameters illustrated in this study on markers for myogenic differentiation.

Subsequently Seahorse assay technology was utilised to explore the effect of a series of wavelengths on real-time mitochondrial respiration. Whilst several studies have explored the effect of specific PBM parameters utilising Seahorse technology (33, 34), ours is the first that has explored an array of wavelengths and in particular the use of blue light in PBM. Our data showed that PBM at all wavelengths upregulated both maximal and basal respiratory rates, ATP production and spare respiratory capacity (the amount of extra ATP produced through oxidative phosphorylation available in the case of an increase in energy demand (35)) in myotubes *(figure 7, $p<0.05$)*, whilst these were only upregulated at a wavelength of 810nm from myoblasts *($p<0.05$)*. Comparatively, previous studies exploring the effects of PBM using a Seahorse analyser only explored the effects of red light (635-700nm) and only *Chu-Tan et al* found PBM modulated real time mitochondrial activity (33). Data from this study suggests that mitochondrial content may influence cellular response to PBM. However, further investigations are required to confirm this finding. Furthermore, our data indicates that blue light promoted greater increases in mitochondrial activity from myotubes compared with NIR irradiation. Interestingly, PBM research does not often employ light within the blue range. However, recently, the application of blue light has gathered considerable interest and several authors have provided evidence that blue light not only could be beneficial in reducing inflammation by reducing circulating levels of cytokines (36) and promoting cell proliferation (37). Hence, in future studies it will be important to explore the response of other cell types to low doses of blue light. However, whilst we have reported blue light induces a greater response compared to NIR light *in vitro,* it may be wise to consider the possible limitations of blue light in terms of tissue penetration depth. Hence, future studies may aim to evaluate the effects of combining both blue and NIR light to ensure light penetrates target tissue *in vivo*. The use of blue light may also be considered for superficial injuries including applications for wound healing, which have proven beneficial both in vitro (38) and in vivo (39, 40).

In summary, we demonstrate for the first time that PBM promotes greater increases in mitochondrial respiration in myotubes compared with myoblasts, a cell type with higher levels of

mitochondrial content. These data may prove useful in understanding why some patients are more responsive to PBM *in vivo* as it is well reported there is a great deal of variability in the mitochondrial genome from one individual to the next (41). We also provide novel evidence that blue light could also be effective in promoting mitochondrial respiration. These data provide further evidence supporting the premise that response to PBM *in vitro* is induced by changes in mitochondrial activity and provides evidence that PBM could be employed to promote increased muscle cell activity. Hence, these data support current findings that indicate the potential effectiveness of PBM in sport performance and rehabilitation following muscle injury (42).

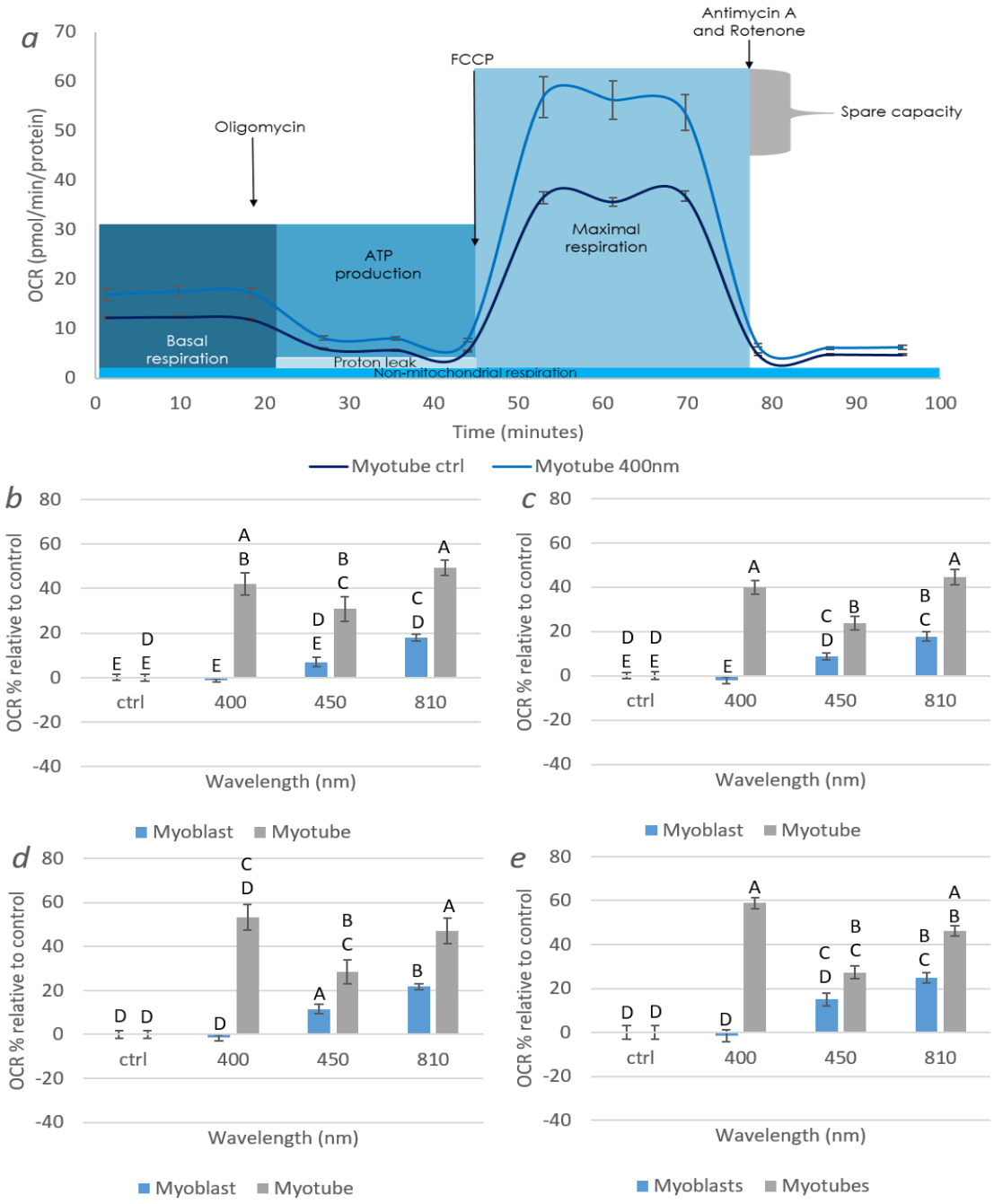

Figure 6: Shows the effects of PBM on markers for changes in real time mitochondrial activity utilising the Seahorse assay from myoblasts and myotubes (myotubes, p7, myoblasts p13, n=6, effects evaluated 8hrs post irradiation). Markers are denoted by a) indicates trace comparing response of untreated myotubes and myotubes treated with 400nm light in which compounds were sequentially applied to the system to alter elements of oxidative phosphorylation. This then enabled calculation of specific parameters of oxidative phosphorylation including b) basal respiration, c) maximal respiration, d) ATP production and e) Spare respiratory capacity. Means that do not share the same letter are significantly different ($p<0.05$).

Acknowledgements

The research in this report is funded as part of an iCASE PHD studentship funded by EPSRC and Philips. The authors declare no potential conflicts of interest with respect to the authorship and/or publication of this article.

4 References

1. Hamblin MR, Demidova TN, editors. Mechanisms of low level light therapy. Progress in Biomedical Optics and Imaging - Proceedings of SPIE; 2006.
2. Yousefi-Nooraie R, Schonstein E, Heidari K, Rashidian A, Pennick V, Akbari-Kamrani M, et al. Low level laser therapy for nonspecific low-back pain. Cochrane Database of Systematic Reviews. 2008(2).
3. Ferraresi C, Huang Y-Y, Hamblin MR. Photobiomodulation in human muscle tissue: an advantage in sports performance? Journal of biophotonics. 2016;9(11-12):1273-99.
4. Woolf AD, Pfleger B. Burden of major musculoskeletal conditions. Bulletin of the World Health Organization. 2003;81(9):646-56.
5. Jenkins PA, Carroll JD. How to report low-level laser therapy (LLLT)/photomedicine dose and beam parameters in clinical and laboratory studies. Photomedicine and Laser Surgery. 2011;29(12):785-7.
6. Karu TI, Kolyakov SF. Exact action spectra for cellular responses relevant to phototherapy. Photomed Laser Surg. 2005;23(4):355-61.
7. Hamblin MR, Demidova-Rice TN, editors. Cellular chromophores and signaling in low level light therapy. Progress in Biomedical Optics and Imaging - Proceedings of SPIE; 2007.
8. Tan B, Xiao H, Xiong X, Wang J, Li G, Yin Y, et al. L-arginine improves DNA synthesis in LPS-challenged enterocytes. Frontiers in bioscience (Landmark edition). 2015;20:989-1003.
9. Piantadosi CA, Carraway MS, Babiker A, Suliman HB. Heme oxygenase-1 regulates cardiac mitochondrial biogenesis via Nrf2-mediated transcriptional control of nuclear respiratory factor-1. Circulation research. 2008;103(11):1232-40.
10. Migliario M, Pittarella P, Fanuli M, Rizzi M, Renò F. Laser-induced osteoblast proliferation is mediated by ROS production. Lasers in Medical Science. 2014;29(4):1463-7.
11. Rhee CK, Chang SY, Ahn JC, Suh MW, Jung JY, editors. Effect of LLLT on the level of ATP and ROS from organ of corti cells. Progress in Biomedical Optics and Imaging - Proceedings of SPIE; 2014.
12. Cole LW. The Evolution of Per-cell Organelle Number. Frontiers in Cell and Developmental Biology. 2016;4:85.
13. Robin ED, Wong R. Mitochondrial DNA molecules and virtual number of mitochondria per cell in mammalian cells. Journal of cellular physiology. 1988;136(3):507-13.
14. Rashid MM, Runci A, Polletta L, Carnevale I, Morgante E, Foglio E, et al. Muscle LIM protein/CSRP3: a mechanosensor with a role in autophagy. Cell death discovery. 2015;1:15014.
15. Bentzinger CF, Wang YX, Rudnicki MA. Building Muscle: Molecular Regulation of Myogenesis. Cold Spring Harbor Perspectives in Biology. 2012;4(2):a008342.
16. Schoneich C, Dremina E, Galeva N, Sharov V. Apoptosis in differentiating C2C12 muscle cells selectively targets Bcl-2-deficient myotubes. Apoptosis : an international journal on programmed cell death. 2014;19(1):42-57.
17. Kraft CS, LeMoine CM, Lyons CN, Michaud D, Mueller CR, Moyes CD. Control of mitochondrial biogenesis during myogenesis. American journal of physiology Cell physiology. 2006;290(4):C1119-27.
18. Hadis MA, Cooper PR, Milward MR, Gorecki PC, Tarte E, Churm J, et al. Development and application of LED arrays for use in phototherapy research. J Biophotonics. 2017.

19. Leggate J, Allain R, Isaac L, Blais BW. Microplate fluorescence assay for the quantification of double stranded DNA using SYBR Green I dye. Biotechnology letters. 2006;28(19):1587-94.
20. Sieuwerts AM, Klijn JG, Peters HA, Foekens JA. The MTT tetrazolium salt assay scrutinized: how to use this assay reliably to measure metabolic activity of cell cultures in vitro for the assessment of growth characteristics, IC50-values and cell survival. European journal of clinical chemistry and clinical biochemistry : journal of the Forum of European Clinical Chemistry Societies. 1995;33(11):813-23.
21. Liu Y, Peterson DA, Kimura H, Schubert D. Mechanism of cellular 3-(4,5-dimethylthiazol-2-yl)-2,5-diphenyltetrazolium bromide (MTT) reduction. Journal of neurochemistry. 1997;69(2):581-93.
22. Gomez-Florit M, Monjo M, Ramis JM. Identification of quercitrin as a potential therapeutic agent for periodontal applications. J Periodontol. 2014;85(7):966-74.
23. Hadis MA, Cooper PR, Milward MR, Gorecki PC, Tarte E, Churm J, et al. Development and application of LED arrays for use in phototherapy research. Journal of Biophotonics. 2017.
24. Nguyen LM, Malamo AG, Larkin-Kaiser KA, Borsa PA, Adhihetty PJ. Effect of near-infrared light exposure on mitochondrial signaling in C2C12 muscle cells. Mitochondrion. 2014;14(1):42-8.
25. Ferraresi C, de Sousa MVP, Huang YY, Bagnato VS, Parizotto NA, Hamblin MR. Time response of increases in ATP and muscle resistance to fatigue after low-level laser (light) therapy (LLLT) in mice. Lasers in Medical Science. 2015;30(4):1259-67.
26. Yang H, Bergmans JWM, Schenk TCW, Linnartz JPMG, Rietman R. An analytical model for the illuminance distribution of a power LED. Optics Express. 2008;16(26):21641-6.
27. Remels AH, Langen RC, Schrauwen P, Schaart G, Schols AM, Gosker HR. Regulation of mitochondrial biogenesis during myogenesis. Molecular and cellular endocrinology. 2010;315(1-2):113-20.
28. Larsen S, Nielsen J, Hansen CN, Nielsen LB, Wibrand F, Stride N, et al. Biomarkers of mitochondrial content in skeletal muscle of healthy young human subjects. The Journal of physiology. 2012;590(14):3349-60.
29. Teuschl A, Balmayor ER, Redl H, van Griensven M, Dungel P. Phototherapy with LED light modulates healing processes in an in vitro scratch-wound model using 3 different cell types. Dermatol Surg. 2015;41(2):261-8.
30. Kushibiki T, Hirasawa T, Okawa S, Ishihara M. Blue laser irradiation generates intracellular reactive oxygen species in various types of cells. Photomedicine and Laser Surgery. 2013;31(3):95-104.
31. Silva LMG, Da Silva CAA, Da Silva A, Vieira RP, Mesquita-Ferrari RA, Cogo JC, et al. Photobiomodulation protects and promotes differentiation of C2C12 myoblast cells exposed to Snake venom. PLoS ONE. 2016;11(4).
32. Shefer G, Ben-Dov N, Halevy O, Oron U. Primary myogenic cells see the light: Improved survival of transplanted myogenic cells following low energy laser irradiation. Lasers in Surgery and Medicine. 2008;40(1):38-45.
33. Chu-Tan JA, Rutar M, Saxena K, Wu Y, Howitt L, Valter K, et al. Efficacy of 670 nm Light Therapy to Protect against Photoreceptor Cell Death Is Dependent on the Severity of Damage. International Journal of Photoenergy. 2016;2016.
34. Wigle JC, Castellanos CC, editors. In vitro measurements of oxygen consumption rates in hTERT-RPE cells exposed to low levels of red light. Progress in Biomedical Optics and Imaging - Proceedings of SPIE; 2016.
35. Desler C, Hansen TL, Frederiksen JB, Marcker ML, Singh KK, Juel Rasmussen L. Is There a Link between Mitochondrial Reserve Respiratory Capacity and Aging? Journal of Aging Research. 2012;2012:192503.
36. Masson-Meyers DS, Bumah VV, Enwemeka CS. Blue light does not impair wound healing in vitro. J Photochem Photobiol B. 2016;160:53-60.

37. Cheon MW, Kim TG, Lee YS, Kim SH. Low level light therapy by Red-Green-Blue LEDs improves healing in an excision model of Sprague-Dawley rats. Personal and Ubiquitous Computing. 2013;17(7):1421-8.
38. Masson-Meyers DS, Bumah VV, Enwemeka CS. Blue light does not impair wound healing in vitro. Journal of Photochemistry and Photobiology B: Biology. 2016;160:53-60.
39. Alba MN, Gerenutti M, Yoshida VMH, Grotto D. Clinical comparison of salicylic acid peel and LED-Laser phototherapy for the treatment of Acne vulgaris in teenagers. Journal of Cosmetic and Laser Therapy. 2017;19(1):49-53.
40. Figurová M, Ledecký V, Karasová M, Hluchý M, Trbolová A, Capík I, et al. Histological Assessment of a Combined Low-Level Laser/Light-Emitting Diode Therapy (685 nm/470 nm) for Sutured Skin Incisions in a Porcine Model: A Short Report. Photomedicine and Laser Surgery. 2016;34(2):53-5.
41. Carter RW. Mitochondrial diversity within modern human populations. Nucleic Acids Research. 2007;35(9):3039-45.
42. Borsa PA, Larkin KA, True JM. Does Phototherapy Enhance Skeletal Muscle Contractile Function and Postexercise Recovery? A Systematic Review. Journal of Athletic Training. 2013;48(1):57-67.